5) Repeat until sufficiently converged.

One complication of IP orbital motion is that the results obtained depend not only on the distance traveled, but also on the direction. In particular, results for translations along the VBAR (the easiest direction to translate along) are significantly different from those for RBAR transfers. However, both the IP and OOP results can be used to quantify the maximum range that is achievable in a given time for a specified acceleration level, by considering transfers with zero-length coast phases. Similarly, they can be used to examine the effect of increasing acceleration level on the total maneuver Δv for transfers between two specified points in a given time. Results will be presented here for IP transfers from the origin to a point along the positive RBAR; the corresponding results for VBAR and OOP transfers are given in Ref. 9.

The maximum distance achievable for transfers along the RBAR is given in Fig. 1. It can be shown to be considerably less than the corresponding distances for transfers along the other two axes; this reflects the difficulty of maneuvering along the RBAR. This difficulty is also demonstrated by the relatively small maximum hover distance, or RBAR hover limit [the maximum radial distance at which the spacecraft is able to station keep by thrusting constantly; from Eq. (1), this distance is $z_h = a/3\omega^2$] of just under 2000 ft for an acceleration of 250 μg. Figure 2 then shows how the maximum maneuver Δv depends on vehicle acceleration; the dashed line in this case shows the value obtained by the standard CW targeting equations for an impulsive vehicle. It can be seen that increasing vehicle acceleration from 250 to 2500 μg leads to a reduction in total maneuver Δv of around 20%; this reduction in the maneuver propellant requirement is quite significant.

Conclusions

This Note has studied low-thrust proximity operations of the type arising with the new class of orbital inspection vehicles. Closed-form expressions were first derived for the trajectory of a spacecraft that is acted upon by a continuous thrust. These were then used as the basis for a numerical procedure for generating a rest-to-rest ACD trajectory that takes a vehicle with a specified acceleration level between two desired points in a specified time. This analysis leads to the following main conclusion: increasing vehicle acceleration by an order of magnitude above the theoretical minimum leads to significantly reduced propellant consumption.

References

[1]"AERCam Sprint Flight Test Project Critical Design Review," NASA Johnson Space Center Automation, Robotics, and Simulation Div., July 1996.

[2]Williams, T. W., and Tanygin, S., "On-Orbit Engineering Tests of the AERCam Sprint Robotic Camera Vehicle," *Proceedings of the AAS/AIAA Spaceflight Mechanics Meeting* (Monterey, CA), Univelt, San Diego, CA, 1998 (American Astronautical Society Paper AAS 98-171, Feb. 1998).

[3]Williams, T. W., and Tanygin, S., "Dynamics of a Near-Symmetrical Spacecraft Driven by a Constant Thrust," *Proceedings of the AAS/AIAA Spaceflight Mechanics Meeting* (Austin, TX), Univelt, San Diego, CA, 1996 (American Astronautical Society Paper AAS 96-160, Feb. 1996).

[4]"Inspector Project Summary," NASA Johnson Space Center Automation, Robotics, and Simulation Div., Aug. 1995.

[5]Kechichian, J. A., "Reformulation of Edelbaum's Low-Thrust Transfer Problem Using Optimal Control Theory," *Journal of Guidance, Control, and Dynamics*, Vol. 20, No. 5, 1997, pp. 988–994.

[6]Clohessy, W. H., and Wiltshire, R. S., "Terminal Guidance System for Satellite Rendezvous," *Journal of the Aerospace Sciences*, Vol. 27, 1960, pp. 653–658.

[7]Kaplan, M. H., *Modern Spacecraft Dynamics and Control*, Wiley, New York, 1976.

[8]Jensen, M. C., Hines, J. M., and Foale, C. M., "Man Overboard Rescue," *Simulation*, Vol. 57, 1991, pp. 39–47.

[9]Williams, T. W., and Tanygin, S., "Trajectory Issues Affecting Propulsion System Sizing and Operations of Orbital Inspection Vehicles," *Proceedings of the AIAA/AAS Astrodynamics Conference* (San Diego, CA), CP969, AIAA, Reston, VA, 1996, pp. 686–696.

Closed-Form Methods for Generating On–Off Commands for Undamped Flexible Spacecraft

William E. Singhose*
Georgia Institute of Technology, Atlanta, Georgia 30332
and
Bart W. Mills† and Warren P. Seering‡
Massachusetts Institute of Technology, Cambridge, Massachusetts 02139

I. Introduction

SEVERAL methods for generating command profiles for flexible spacecraft have recently been proposed.[1–7] Many of these techniques have been directed toward systems equipped with on–off reaction jets. Using the commands generated by these methods, a flexible spacecraft can be moved with small levels of residual vibration. Furthermore, the commands can be robust to modeling errors,[2,4,8] limit transient deflection,[5] and limit fuel consumption.[6] Although these techniques are powerful, they have the drawback that a separate numerical optimization must be performed to generate the command for every unique motion. This drawback introduces a time delay at the start of every motion, or requires the command profiles to be precomputed and stored for retrieval.

Consider rest-to-rest slewing of a two-mass and spring system where the control force acts on the first mass m_1. To account for the case of on–off actuators, the force is restricted to values of $u_{\max}$, 0, and $-u_{\max}$. If all system parameters (m_1, m_2, k, $u_{\max}$) are set equal to 1, then the system has a natural frequency of $\sqrt{2}$ rad/s and a force-to-mass ratio of 0.5.

Designing a bang-bang command profile (the simplest on–off command) to move the benchmark system, a desired distance is straightforward. If we assume that the bang-bang command begins at time zero, then the only unknown is the switch time t_2 because the duration of the negative pulse must equal the duration of the positive pulse to bring the system to rest. The value of t_2 can be obtained from the rigid-body dynamics as

$$t_2 = \sqrt{x_d/\alpha} \tag{1}$$

where x_d is the desired move distance and $\alpha = u_{\max}/(m_1 + m_2)$ is the force-to-mass ratio. The bang-bang command moves the center of mass to the desired position, but significant residual oscillations will usually exist when the system has flexibility. However, the bang-bang command has the advantage of being completely described by the simple expression given in Eq. (1).

By taking into account the system flexibility, time-optimal and near time-optimal command profiles can be generated to eliminate the residual vibration.[1–6,8] The time-optimal open-loop command profiles for linear systems are multiswitch bang-bang commands that must be obtained using a numerical optimization. The rise time is slower than with the bang-bang command, but the residual oscillation is eliminated. The development of time-optimal flexible-body commands will not be explained here, but we emphasize that

Received Oct. 23, 1997; revision received Oct. 18, 1998; accepted for publication Oct. 30, 1998.

*Assistant Professor, Department of Mechanical Engineering. Member AIAA.

†Research Assistant, Department of Mechanical Engineering.

‡Professor, Department of Mechanical Engineering.

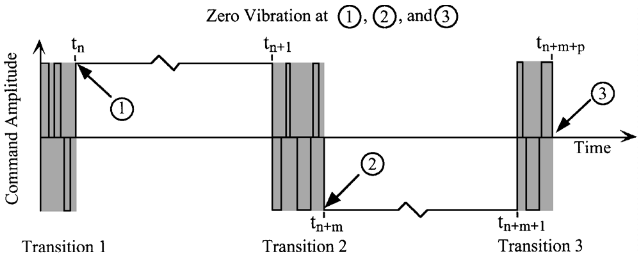

Fig. 1 Generating an on–off command using transition shaping.

a numerical optimization is required to obtain the switch times of the command for each unique motion. Additionally, methods that verify the results of the required numerical optimization must be used to ensure consistent performance.[8]

The goal of this work is to eliminate the need for numerical optimization when generating on–off command profiles for flexible spacecraft. Commands that can be described by simple functions of the system frequencies, the desired move distance, and the force-to-mass ratio will be developed.

The vibration induced by a bang-bang command results from the three step transitions in the actuator state: 1) zero to positive, 2) positive to negative, and 3) negative to zero. Because a bang-bang command gives a rapid rigid-body response, the procedure proposed here forms a pseudo-bang-bang command whose transitions do not cause residual vibration.

The command generation method consists of two phases. First, segments of the command profile are generated so that they accelerate the system without causing residual vibration. We emphasize that these segments are not entire command profiles, but rather they cause changes in the actuator state without causing residual vibration. In the second phase the command segments are combined with periods of constant acceleration to form the entire command profile. The flexible dynamics of the system are canceled by the actuator state transitions. The rigid-body requirements are then taken into account by specifying the time between the actuator state transitions. This two-step process will be referred to as transition shaping and is shown schematically in Fig. 1. For this general case the first transition contains n switches, the second has m switches, and the third has p switches.

The method proposed here has similarities to control methods developed previously for moving suspended payloads.[9–11] The previous methods generated on–off commands that accelerated suspended payloads up to constant velocity and then decelerated them without residual vibration. The commands developed here are not for constant velocity motion, but rather the commands accelerate the system up to the midpoint of the maneuver and then decelerate to a rest position. Additionally, the technique presented here can be made robust to modeling errors, can handle multiple modes of vibration, and can produce fuel-efficient command profiles.

II. Command Generation for Single-Mode Systems

A. One-Unit Transitions

There are several methods of transitioning an on–off actuator state from zero to positive without causing residual vibration. One simple way to accomplish such a transition is to turn the actuator on for $T/6$ seconds, where T is the period of system vibration, turn the actuator off for $T/6$ seconds, and then turn the actuator back on. Such a command transition is shown in the upper right part of Fig. 2a. The vibration induced by the three switches adds up to zero. This can be better understood by interpreting the transition as a step function convolved with a sequence of impulses given by[12]

$$\begin{bmatrix} A_i \\ t_i \end{bmatrix} = \begin{bmatrix} 1 & -1 & 1 \\ 0 & T/6 & T/3 \end{bmatrix} \tag{2}$$

where A_i and t_i are the impulse amplitudes and time locations. By superimposing the response (of our benchmark system) from each of the three impulses given in Eq. (2), one finds that the total response has zero residual vibration.[12]

The process of convolving an impulse sequence with a step function to generate an on–off command profile can be considered a special case of input shaping, and the impulse sequence is called an input shaper.[13] Given that the input shaper described by Eq. (2) yields zero residual vibration, then the command formed by convolving the shaper with a step input will also lead to zero residual vibration.[13] The shaper given in Eq. (2) does not generate the fastest possible transition; however, it is of interest because it does not produce negative pulses. Note that the shaper contains a negative impulse, but the resulting transition (the convolution product shown in Fig. 2a) does not contain a negative pulse. Consequently, this is a fuel-efficient transition.[6] The time-optimal transition requires a negative pulse and can be obtained by using an input shaper described by[12]

$$\begin{bmatrix} A_i \\ t_i \end{bmatrix} = \begin{bmatrix} 1 & -2 & 2 \\ 0 & \dfrac{\cos^{-1}(1/4)}{2\pi}T & \dfrac{\cos^{-1}(-1/4)}{2\pi}T \end{bmatrix}$$
$$= \begin{bmatrix} 1 & -2 & 2 \\ 0 & 0.20978T & 0.29022T \end{bmatrix} \tag{3}$$

When the system model is not exact, the command transition produced by either Eq. (2) or (3) will result in some finite amount of residual vibration. As the actual frequency deviates from the modeling frequency, the amplitude of residual vibration increases rapidly. This result has motivated the development of robust input shapers. A robust time-optimal shaper is given by[12]

$$\begin{bmatrix} A_i \\ t_i \end{bmatrix} = \begin{bmatrix} 1 & -2 & 2 & -2 & 2 \\ 0 & 0.1524T & 0.2774T & 0.6313T & 0.679T \end{bmatrix} \tag{4}$$

If Eq. (4) is used to generate an actuator state transition, then the vibration remains small even when the actual frequency deviates

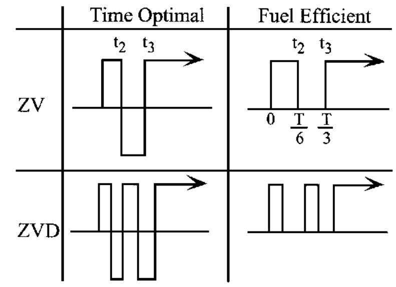

Transition	t_2	t_3	t_4	t_5
ZV-TO	0.20978T	0.29022T	—	—
ZV-FE	T/6	T/3	—	—
ZVD-TO	0.15241T	0.27740T	0.63131T	0.67895T
ZVD-FE	0.08951T	0.36623T	$2t_3{-}t_2$	$2t_3$

a) One-unit transitions

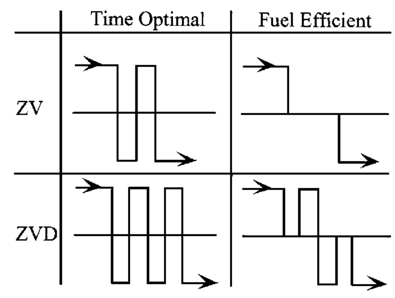

Transition	t_2	t_3	t_4	t_5
ZV-TO	T/6	T/3	—	—
ZV-FE	T/2	—	—	—
ZVD-TO	0.08951T	0.36623T	$2t_3{-}t_2$	$2t_3$
ZVD-FE	0.18434T	0.40882T	$2t_3{-}t_2$	$2t_3$

b) Two-unit transitions

Fig. 2 Actuator state transitions.

considerably from the modeling frequency. The robustness is obtained by forcing the derivative of the residual vibration amplitude equal to zero at the modeling frequency.[13]

Four possible transitions from zero to a positive actuator state are shown in Fig. 2a. The nonrobust transitions are in the top row and are labeled zero vibration (ZV) because they are designed by only requiring zero residual vibration. The robust transitions are labeled zero vibration and derivative (ZVD) because the zero derivative constraint is also satisfied. The columns are further labeled time optimal (TO) or fuel efficient (FE), where the key difference is that the FE transitions do not contain negative pulses. These one-unit transition functions also can be used to go from negative to zero actuator effort by simply reversing the transition.

B. Two-Unit Transitions

The first and third transitions of a pseudo-bang-bang command can be generated with the functions shown in Fig. 2a. However, the second transition of the command (positive to negative) is different because it is a change of two units ($2u_{\max}$). The simplest vibration-free transition from positive to negative can be accomplished with only two switches. The actuator is turned off, the system coasts for $T/2$, and then the actuator state is turned negative. This is the ZV FE transition and is one of the four possible two-unit transitions shown in Fig. 2b.

C. Complete Command Profiles

The transition functions shown in Fig. 2 can be used in a simple two-step process to generate command profiles that perform rest-to-rest motion. First, a shaper is selected for each of the three transitions in the pseudo-bang-bang command. Second, the necessary time between transitions is determined from the rigid-body requirements.

To demonstrate this process, commands for ZV FE motion will be designed. The first and third transitions will use the one-unit ZV FE transition from Fig. 2a. The middle transition will be performed with the two-unit ZV FE transition of Fig. 2b. A command profile will be described by its three transitions. The command under consideration is then a ZV FE-FE-FE command. This command is antisymmetric and can be described as

$$\begin{bmatrix} A_i \\ t_i \end{bmatrix} = \begin{bmatrix} 1 & -1 & 1 & -1 & -1 & 1 & -1 & 1 \\ t_1 & t_2 & t_3 & t_4 & t_5 & t_6 & t_7 & t_8 \end{bmatrix} \tag{5}$$

For antisymmetric commands only the switch times up through midmaneuver t_m need to be determined. In this case t_m lies directly between t_4 and t_5. For the ZV FE-FE-FE command, t_2, t_3, t_4, and t_5 must be determined ($t_1 = 0$). From Fig. 2a t_2 and t_3 are known to be $T/6$ and $T/3$, respectively. From Fig. 2b the spacing between t_4 and t_5 is known to be $T/2$. Therefore,

$$t_m = t_4 + (T/4) \tag{6}$$

The value of t_4 is now determined from rigid-body mechanics. At midmaneuver the position of the center of mass x_{tm} must be at one half of the desired move distance. By simply integrating the rigid-body equation of motion with respect to time, an expression for the mass center position as a function of the switch times is obtained:

$$x_{tm} = x_d/2 = (\alpha/2)\left[-t_2^2 + t_3^2 - t_4^2\right] + \alpha t_m[t_2 - t_3 + t_4] \tag{7}$$

Using Eqs. (6) and (7) and the known values of t_2 and t_3, t_4 is found to be

$$t_4 = (-T/12) + \sqrt{(T/12)^2 + (x_d/\alpha)} \tag{8}$$

By symmetry, the entire ZV FE-FE-FE command is now known to be given as

$$\begin{bmatrix} A_i \\ t_i \end{bmatrix} = \begin{bmatrix} 1 & -1 & 1 & -1 & -1 & 1 & -1 & 1 \\ 0 & T/6 & T/3 & \left[(-T/12) + \sqrt{(T/12)^2 + (x_d/\alpha)}\right] & t_4 + (T/2) & t_5 + t_4 - t_3 & t_5 + t_4 - t_2 & t_5 + t_4 \end{bmatrix} \tag{9}$$

An on–off command can be generated by simply substituting the system parameters into Eq. (9). As expected, the closed-form commands are slower than the time-optimal commands. This drawback is obviously countered by the ease of generating the closed-form commands. What is not obvious thus far are the advantages provided by the closed-form commands in terms of fuel savings, robustness to modeling errors, and decreased maximum transient deflection. These will be discussed in Sec. III.

Before proceeding with the design of commands involving other combinations of transitions, it should be noted that the closed-form commands cannot be used for very small move distances. A problem occurs because the time durations of the three transitions are fixed by the flexible-body dynamics. The minimum move distance occurs when the three transitions occur sequentially without delay. For the ZV FE-FE-FE command the minimum move distance occurs when $t_4 = t_3$. Using this condition, the minimum move distance for the ZV FE-FE-FE command can be calculated as

$$[x_{\min}]_{\text{ZV FE-FE-FE}} = (\alpha/6)T^2 = 0.16667\alpha T^2 \tag{10}$$

For the benchmark system the minimum move distance using the ZV FE-FE-FE command is 1.645 units. As an alternate form for expressing this constraint, the minimum move time can be calculated. In this case moves lasting less than $\frac{7}{6}$ of the vibration period cannot be performed.

To decrease the minimum move distance and improve the rise time, time-optimal transitions can be used. The design of the ZV TO-TO-TO command proceeds in exactly the same manner as for the ZV FE-FE-FE command, except that the time-optimal transitions from Fig. 2 are used. The time-optimal transitions produce only a very small improvement in rise time while causing a significant increase in fuel usage (the time the actuator effort is nonzero). A similar effect has been noted previously for numerically obtained commands.[6] The main advantage of time-optimal transitions is that they allow for smaller move distances. In this case $x_{\min} = 0.086627\alpha T^2$.

Note the significant decrease in the minimum move distance as compared to that given in Eq. (10) for the ZV FE-FE-FE command. At this point we reiterate that transition shaping does not produce time-optimal commands. The ZV TO-TO-TO command uses time-optimal transitions, but it is not the time-optimal command that moves the system with zero residual vibration.

As mentioned previously, ZV commands are not robust to modeling errors. Robust shapers, such as the ZVD shapers, must be used on most real systems. The ZVD FE-FE-FE command is given by

$$\begin{gathered} A_i = [1 \quad -1 \quad 1 \quad \cdots \quad 1 \quad -2 \quad 1 \quad -1 \quad \cdots \quad 1] \\ t_2 = 0.08951T, \qquad t_3 = 0.36623T \\ t_4 = 2t_3 - t_2, \qquad t_5 = 2t_3 \\ t_6 = -0.04259T + \sqrt{(0.04051T)^2 + (x_d/\alpha)} \\ t_7 = t_6 + 0.099161T, \qquad t_8 = t_6 + 0.323643T \\ t_9 \rightarrow t_{15}\text{: by symmetry}, \qquad x_{\min} = 0.599075\alpha T^2 \end{gathered} \tag{11}$$

There are a great variety of commands that can be designed with transition shaping. For example, an asymmetrical command such as a ZV TO-FE-FE command can be designed, or a command with both ZV and ZVD constraints can be constructed.

III. Comparison of Single-Mode Commands

When designing command profiles for flexible spacecraft, there are several tradeoffs that must be considered. Rapid motion is desired, but fuel usage, maximum transient deflection, and robustness to modeling errors also must be within acceptable bounds. This section evaluates these quantities for the closed-form commands, and comparisons will be made to time-optimal commands obtained using numerical optimization. As mentioned previously, commands using time-optimal transitions are usually poor alternatives to commands containing fuel-efficient transitions because they improve maneuver speed only slightly while requiring a large increase in fuel expenditure. Therefore, this section will only compare closed-form, fuel-efficient commands to time-optimal commands.

A. Move Duration

The duration of a move is usually defined as the length of time from the start of motion to the point when the vibration has settled to within a tolerable level. When using shaped commands to eliminate residual vibration, the settling time coincides with the length of the command. The ZV FE-FE-FE command averages only 9.4% longer than the TO ZV command over the range $10 \le x_d \le 40$. The ZVD FE-FE-FE commands average 15% longer than the TO ZVD command. The percentage increase in move time with the closed-form commands decreases with move distance. Therefore, they become more attractive solutions as the move distance increases.

B. Fuel Usage

The amount of fuel used during the slewing of flexible spacecraft is very important. The fuel usage (measured by the time duration the actuators are turned on) of the time-optimal commands is equal to the move duration because the actuators are turned on throughout the motion. The closed-form commands always use less fuel than the time- optimal commands. The ZV FE-FE-FE command uses an average of 16.8% less fuel than the TO ZV command, whereas the ZVD FE-FE-FE uses an average of 17.7% less fuel than the TO ZVD command over the range $10 \le x_d \le 40$.

C. Maximum Transient Deflection

Another important consideration is the maximum deflection that occurs during the motion. The shaped commands control the residual vibration, but no provision is made for limiting the transient deflection. Techniques for limiting maximum transient deflection have been developed[5] but will not be treated here. The deflection for the benchmark system is defined as the position of m_2 minus the position of m_1 ($|x_2 - x_1|$). The closed-form commands cause a maximum deflection of 0.5 units, whereas the TO ZV commands cause twice as much deflection for most moves. The TO ZVD command leads to maximum deflections in the 0.5 to 1.0 range. Without directly addressing the problem the closed-form commands significantly reduce the transient deflection as compared to time-optimal commands.

D. Robustness to Modeling Errors

All of the commands under consideration produce motion with zero residual vibration provided that the system model is perfect. When the model is imperfect, the amplitude of residual vibration is highly dependent on the command. The ZVD commands are much more robust than the ZV commands; however, the level of robustness is dependent on the move distance and the type of command. For example, the TO ZVD command is much less robust than the ZVD FE-FE-FE command. Using a measure of robustness called insensitivity,[12] the ZV FE-FE-FE command averages 450% more robustness than the TO ZV command over the range of move distances up to $x_d = 40$. The ZVD FE-FE-FE command averages 360% more robustness than the TO ZVD command.

The large increases in robustness provided by the closed-form commands warrant some explanation. Any type of on–off command eliminates vibration by summing to zero the vibration caused by each switch in the command. Time-optimal commands perform this cancellation only at the end of the maneuver, so the final switch must cancel the vibration caused by all of the previous switches. The closed-form commands do not wait until the end of the maneuver to cancel vibration; each transition results in zero residual vibration.

For example, assume that the modeling frequency is 10% higher than the actual frequency. The time locations of the switches in the ZV FE-FE-FE command will be incorrect by 10%. Examining the middle transition (positive to negative), we see that the period between t_4 and t_5 is one half period of the modeling frequency. That is, t_5 occurs after the vibration from t_4 has completed 180 deg of its cycle. Given that the actual period is 10% longer than the modeling period, t_5 occurs after the vibration induced at t_4 has completed only 164 deg of its cycle; t_5 is incorrect by 16 deg. This type of analysis is also applicable to the first and third transitions; each of the switches in the entire command is, at most, 16 deg away from the intended location.

Under the same examination a very different result is obtained for time-optimal commands. Consider the TO ZV command for $x_d = 5$. The final impulse t_5 is located at 1.5 periods of the modeling frequency; it should occur 540 deg after the first impulse. Given the same 10% modeling error used in the preceding paragraph, t_5 occurs 491 deg after the first impulse; it is incorrect relative to the first impulse by 49 deg. Because time-optimal commands do not cancel vibration until the final impulse, any modeling error will be multiplied by the number of vibration cycles that occur during the slew. Given that the closed-form commands cancel vibration well within one cycle of the vibration, modeling errors do not multiply, and robustness is greatly improved.

IV. Command Generation for Multimode Systems

The process of transition shaping can be extended in a straightforward manner to multimode systems. The same basic two-step process is used; however, analytic formulas do not exist for multimode on–off transitions. Furthermore, it is not generally possible to take single-mode shapers and convolve them together to form a multimode shaper. If this convolution is done, then the convolved input shaper could contain several positive (or negative) impulses in sequence. When convolved with a step input, this shaper would lead to a command profile that exceeds the actuator bounds of $\pm u_{\max}$.

For the multimode case, the transitions must be obtained through the one time use of a numerical optimization. Once the transitions are obtained, commands can be generated for any move distance without having to perform additional numerical optimizations. For antisymmetric profiles the beginning of the second transition t_β is given by

$$
\begin{aligned}
t_\beta = {} & [-t_2 + t_3 - \cdots + t_{n-1} - 0.5(t_y + t_z)] \\
& + \sqrt{\begin{aligned} & 2\left(t_2^2 + t_4^2 + \cdots t_{n-2}^2\right) + \left[-t_a^2 + t_b^2 - t_c^2 \cdots + 0.25 * \left(t_y^2 + t_z^2\right)\right] + 2t_2(-t_3 + t_4 \cdots - t_{n-1}) + 2t_3(-t_4 + t_5 \cdots + t_{n-1}) \\ & + 2t_4(-t_5 + t_6 \cdots - t_{n-1}) \cdots - t_{n-2}(t_{n-1}) - 0.5t_y t_z + t_y(t_a - t_b + t_c \cdots + t_{y-1}) + t_z(t_a - t_b + t_c \cdots + t_{y-1}) + (x_d/\alpha) \end{aligned}}
\end{aligned} \tag{12}
$$

where t_y and t_z are the middle times of the second transition. Once t_β is calculated, the complete profile is determined by using the same time spacing between the second and third transitions.

V. Simulation Results

To demonstrate the process of transition shaping on a complex flexible system, simulations were performed using Draper Laboratory's computer model (the DRS) of the Space Shuttle and its telerobotic manipulator (the RMS). The DRS was developed over a period of 10 years and has been verified numerous times with actual Shuttle flight data. The simulations performed for this Note include

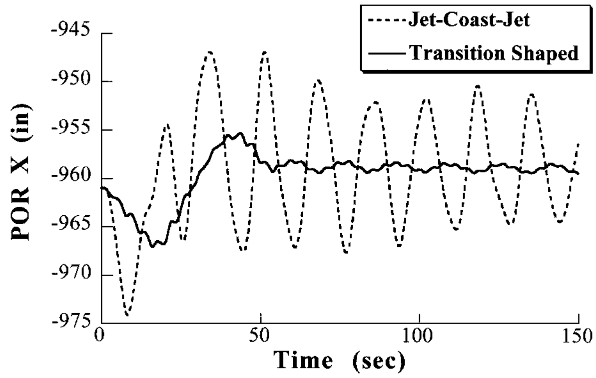

Fig. 3 Endpoint response to jet-coast-jet and transition-shaped command profiles.

a model of the Hubble Space Telescope deployed on the RMS in the extended park position. The simulations reorient the system by firing the Shuttle's reaction jets.

The first simulation fired a jet for approximately 15 s, let the system coast for 8 s, and then fired a roughly opposing jet for 15 s to decelerate the system. The second simulation used a ZVD closed-form command profile designed to perform the same rigid-body motion. The actuator state transitions were generated to suppress the two most important modes of the system, 0.065 and 0.134 Hz. Figure 3 compares the system response to both the jet-coast-jet and the transition-shaped command profiles. The data plotted in Fig. 3 is the POR (Point of Resolution) X coordinate. The POR is a position vector from the tip of the manipulator to a point fixed in the rigid-body reference frame of the Space Shuttle. Using the jet-coast-jet command, the endpoint oscillation is over 20 in. With the transition-shapedcommand profile the residual oscillation is reduced to less than 1.5 in., well over an order of magnitude reduction.

VI. Conclusions

A closed-form method for generating on–off commands for flexible spacecraft was presented. The commands offer considerable advantages over time-optimal commands in terms of fuel usage, transient deflection, and robustness to modeling errors. The cost of these advantages is a modest increase in the slew duration. The most significant advantage provided by the new commands is their ease of design and implementation.

Acknowledgments

Support for this work was provided by MIT's Lincoln Laboratory through Grant BX-6473 and MIT's Undergraduate Research Opportunities Program.

References

[1]Ben-Asher, J., Burns, J. A., and Cliff, E. M., "Time-Optimal Slewing of Flexible Spacecraft," *Journal of Guidance, Control, and Dynamics*, Vol. 15, No. 2, 1992, pp. 360–367.

[2]Liu, Q., and Wie, B., "Robust Time-Optimal Control of Uncertain Flexible Spacecraft," *Journal of Guidance, Control, and Dynamics*, Vol. 15, No. 3, 1992, pp. 597–604.

[3]Pao, L. Y., "Minimum-Time Control Characteristics of Flexible Structures," *Journal of Guidance, Control, and Dynamics*, Vol. 19, No. 1, 1996, pp. 123–129.

[4]Singh, T., and Vadali, S. R., "Robust Time-Optimal Control: A Frequency Domain Approach," *Journal of Guidance, Control, and Dynamics*, Vol. 17, No. 2, 1994, pp. 346–353.

[5]Singhose, W., Banerjee, A., and Seering, W., "Slewing Flexible Spacecraft with Deflection-Limiting Input Shaping," *Journal of Guidance, Control, and Dynamics*, Vol. 20, No. 2, 1997, pp. 291–298.

[6]Singhose, W., Bohlke, K., and Seering, W., "Fuel-Efficient Pulse Command Profiles for Flexible Spacecraft," *Journal of Guidance, Control, and Dynamics*, Vol. 19, No. 4, 1996, pp. 954–960.

[7]Gorinevsky, D., and Vukovich, G., "Nonlinear Input Shaping Control of Flexible Spacecraft Reorientation Maneuver," *Journal of Guidance, Control, and Dynamics*, Vol. 21, No. 2, 1998, pp. 264–270.

[8]Pao, L. Y., and Singhose, W. E., "Verifying Robust Time-Optimal Commands for Multi-Mode Flexible Spacecraft," *Journal of Guidance, Control, and Dynamics*, Vol. 20, No. 4, 1997, pp. 831–833.

[9]Jones, J. F., and Petterson, B. J., "Oscillation Damped Movement of Suspended Objects," IEEE International Conf. on Robotics and Automation, Philadelphia, PA, Vol. 2, 1988, pp. 956–962.

[10]Noakes, M. W., and Jansen, J. F., "Generalized Inputs for Damped-Vibration Control of Suspended Payloads," *Robotics and Autonomous Systems*, Vol. 10, No. 2, 1992, pp. 199–205.

[11]Starr, G. P., "Swing-Free Transport of Suspended Objects with a Path-Controlled Robot Manipulator," *Journal of Dynamic Systems, Measurement, and Control*, Vol. 107, March 1985, pp. 97–100.

[12]Singhose, W., Singer, N., and Seering, W., "Time-Optimal Negative Input Shapers," *Journal of Dynamic Systems, Measurement, and Control*, Vol. 119, June 1997, pp. 198–205.

[13]Singer, N. C., and Seering, W. P., "Preshaping Command Inputs to Reduce System Vibration," *Journal of Dynamic Systems, Measurement, and Control*, Vol. 112, March 1990, pp. 76–82.